Hong-Hong Zhang, Ji Hu, You-Lang Zhou, Xin Qin, Zhen-Yuan Song, Pan-Pan Yang, Shufen Hu, Xinghong Jiang, and Guang-Yin Xu

Promoted Interaction of Nuclear Factor-κB With Demethylated Purinergic P2X3 Receptor Gene Contributes to Neuropathic Pain in Rats With Diabetes

Diabetes 2015;64:4272–4284 | DOI: 10.2337/db15-0138

Painful diabetic neuropathy is a common complication of diabetes produced by mechanisms that as yet are incompletely defined. The aim of this study was to investigate the roles of nuclear factor-κB (NF-κB) in the regulation of purinergic receptor P2X ligand-gated ion channel 3 (P2X3R) plasticity in dorsal root ganglion (DRG) neurons of rats with painful diabetes. Here, we showed that hindpaw pain hypersensitivity in streptozocin-induced diabetic rats was attenuated by treatment with purinergic receptor antagonist suramin or A-317491. The expression and function of P2X3Rs was markedly enhanced in hindpaw-innervated DRG neurons in diabetic rats. The CpG (cytosine guanine dinucleotide) island in the *p2x3r* gene promoter region was significantly demethylated, and the expression of DNA methyltransferase 3b was remarkably downregulated in DRGs in diabetic rats. The binding ability of p65 (an active form of NF-κB) with the *p2x3r* gene promoter region and p65 expression were enhanced significantly in diabetes. The inhibition of p65 signaling using the NF-κB inhibitor pyrrolidine dithiocarbamate or recombinant lentiviral vectors designated as lentiviral vector-p65 small interfering RNA remarkably suppressed P2X3R activities and attenuated diabetic pain hypersensitivity. Insulin treatment significantly attenuated pain hypersensitivity and suppressed the expression of p65 and P2X3Rs. Our findings suggest that the *p2x3r* gene promoter DNA demethylation and enhanced interaction with p65 contributes to P2X3R sensitization and diabetic pain hypersensitivity.

The lifetime incidence of diabetic neuropathy is 54–59% for patients with type 1 diabetes and 45–70% for patients with type 2 diabetes (1,2). The most common form of diabetic neuropathy is nerve damage in the periphery. Painful diabetic neuropathy develops in about a third of patients with diabetic peripheral neuropathy, who experience aberrant pain sensation, including spontaneous pain, hyperalgesia, and allodynia (3,4). Although several analgesic drugs, such as duloxetine and pregabalin, recently have been used in clinical practice, the pharmacological treatment of chronic painful diabetic neuropathy remains a challenge for the physician, partly because of our poor understanding of the molecular mechanisms underlying diabetic neuropathic pain (5,6).

Recent studies (7–9) have suggested the involvement of some ion channels or receptors in dorsal root ganglion (DRG) neurons in diabetic neuropathic pain in rats. Voltage-gated sodium channel $Na_V1.7$ expression was significantly increased in L4–L6 DRG neurons of rats with diabetic neuropathic pain (7,10). Transient receptor potential vanilloid 1 receptors are also thought to contribute to changes in the activity of DRG neurons under diabetic conditions (11). More recently, others and we have reported that the purinergic P2X receptor (P2XR) antagonists reduced pain behaviors in diabetic mice (12) and rats (13). ATP, an endogenous ligand for purinergic P2XRs, is present in abundance within neuronal and glial cells (14). It is released upon cell stress, stimulation, or damage, thus activating P2XRs present in sensory afferent endings to produce

Jiangsu Key Laboratory of Translational Research and Therapy for Neuro-Psycho-Diseases, Institute of Neuroscience, The Second Affiliated Hospital, Soochow University, Suzhou, People's Republic of China

Corresponding author: Guang-Yin Xu, guangyinxu@suda.edu.cn, or Ji Hu, huji@suda.edu.cn.

Received 30 January 2015 and accepted 24 June 2015.

This article contains Supplementary Data online at http://diabetes.diabetesjournals.org/lookup/suppl/doi:10.2337/db15-0138/-/DC1.

H.-H.Z., J.H., and Y.-L.Z. contributed equally to this study.

See accompanying article, p. 3987.

pain (15). Purinergic P2X ligand-gated ion channel 3 receptors (P2X3Rs) and P2X2Rs/P2X3Rs are preferentially expressed in DRG neurons and are upregulated under neuropathic (16–18), inflammatory (19), and visceral pain hypersensitivity conditions (20). However, the underlying mechanism by which *p2xr* gene expression is upregulated remains unknown under diabetic conditions.

Nuclear factor-κB (NF-κB), a nuclear transcription factor, is considered to control numerous genes encoding inflammatory and nociceptive mediators and to play roles in the development of thermal hyperalgesia after chronic compression of the DRG in rats (21,22). Our previous work (9,23) has demonstrated that p65 (a subunit of NF-κB) expression was upregulated in the DRGs of diabetic rats that are in pain and that the inhibition of p65 subunits by pyrrolidine dithiocarbamate (PDTC) (an inhibitor of NF-κB that inhibits the inhibitor of κB [IκB] phosphorylation) significantly alleviated mechanical allodynia of the rat hindpaw. However, whether p65 regulated P2X3R function and expression remains unclear. Therefore, we hypothesized that streptozocin (STZ)–induced diabetes led to demethylation of *p2x3r* gene promoter DNA and promoted p65 binding to the demethylated *p2x3r* gene promoter, thus resulting in the upregulation of P2X3R expression and diabetic pain hypersensitivity. To test this hypothesis, we constructed a lentiviral vector (LV) encoding a specially designed small interfering RNA (siRNA) against p65 gene (LV-p65) and observed the inhibitory effects of in vivo intrathecal delivery of LV siRNA. Our data demonstrate for the first time, to the best of our knowledge, that STZ-induced diabetes promoted p65 binding to the *p2x3r* gene promoter region. Selective blockade of p65 by PDTC or siRNA attenuates diabetes-induced painful behaviors via the inhibition of P2X3R activities of lumber DRG neurons that innervate the hindpaws. Therefore, selective inhibition of p65 represents a novel potential target for diabetic neuropathic pain therapy.

RESEARCH DESIGN AND METHODS

Generation of STZ-Induced Diabetic Rats

All experiments were approved by the Institutional Animal Care and Use Committee at Soochow University. Adult female Sprague-Dawley (SD) rats weighing 150–180 g were housed four per cage under a 12-h light-dark cycle and in a temperature-controlled room (25 ± 1°C). Rats were allowed access to tap water and standard laboratory chow ad libitum. The diabetic model was induced by a single intraperitoneal injection of STZ (65 mg/kg; Sigma-Aldrich, St. Louis, MO), as described previously (9,13). The average blood glucose levels are shown in Supplementary Table 1. Only rats with a blood glucose concentration of >15.0 mmol/L (270 mg/dL) were further used in the study.

Measurement of Hindpaw Withdrawal Threshold

All animals were habituated to the test environment for 1 week prior to testing. The pain threshold was determined before and after an injection of STZ or normal saline (NS). Rat paw withdrawal threshold (PWT) in response to the von Frey filament stimulation and thermal paw withdrawal latency (PWL) in response to radiant heat application to the plantar surface of the hindpaw were determined as described previously (13,23–25). All behavioral studies were performed under blind conditions.

Cell Retrograde Labeling

The origin of the primary afferent innervation of the hindpaw was determined by retrograde tracing using 1,19-dioleyl-3,3,39,3-tetramethylindocarbocyanine methanesulfonate (DiI; Invitrogen, Carlsbad, CA), as described previously (13,26).

Dissociation of DRG Neurons and Patch-Clamp Recordings

Isolation of DRG neurons from adult SD rats was described previously (9,19). DiI-labeled neurons were identified under an inverting fluorescence microscope (model IX71; Olympus, Tokyo, Japan). ATP-evoked currents were recorded by whole-cell patch-clamp recordings in a voltage-clamped mode, as described previously (13).

Western Blotting Analysis

The expressions of P2XRs (P2X1, P2X2, and P2X3) and p65 in L4–L6 DRGs from control and diabetic rats with or without insulin treatment were measured using Western blot analyses (9,13). Anti-p65 (1:500; Abcam, Hong Kong) and anti-P2XRs (1:1,000; Abcam, Cambridge, MA) and corresponding horseradish peroxidase–conjugated secondary anti-rat antibodies at dilutions of 1:2,000 and 1:4,000 were used to probe the proteins.

Real-Time PCR

The mRNA expressions of p65, P2X3R, and DNA methylation-related enzymes were measured using real-time PCR (RT-PCR), as described previously (9,27). Total RNA was extracted from L4–L6 DRGs with TRIzol (Invitrogen), and cDNA was synthesized from total RNA using an Omniscript RT kit 150 (QIAGEN) following the instructions of the supplier. The sequences of the specific primers are shown in Table 1.

Immunofluorescence Study

Triple labeling was performed as described previously (9,28). DiI was injected into the plantar skin of bilateral hindpaws to label hindpaws innervating DRG neurons. p65 (1:100) and P2X3R (1:200) antibodies were used in the current study.

Methylation-Specific PCR and Bisulfite Sequencing

The methylation status of the cytosine guanine dinucleotide (CpG) islands of all samples was initially screened at *p2x3r* gene promoter regions by methylation-specific PCR (MSP), as described previously (27). The MSP primers designed for P2X3R are shown in Table 1. The methylation status was further validated by bisulfite sequencing,

Table 1—Oligonucleotides used in the study

Usage	Primers	Sequence (5′ to 3′)
RT-PCR	P2X3R-F	CCAGTGCATCCCTAAATATTCC
	P2X3R-R	CCAGCGTTCCCATATACCAG
	DNMT3a-F	GAGGGAACTGAGACCCCAC
	DNMT3a-R	CTGGAAGGTGAGTCTTGGCA
	DNMT3b-F	CATAAGTCGAAGGTGCGTCGT
	DNMT3b-R	ACTTTTGTTCTCGCGTCTCCT
	TDG-F	AGGTGTGTGTGGCAGATGGTT
	TDG-R	CCTACTGTGTTCTCAGGAGCCTAC
	Gadd45a-F	CAAGCAGTCACTCCCCACG
	Gadd45a-R	CCTTCAGTCTCACCTCTCTCTCC
	MBD2-F	AAGAACCCTGCTGTTTGGCT
	MBD2-R	TTCTTTCGGACTTGTTGGACTC
	MBD4-F	AATATGGCAACGACTCCTACCG
	MBD4-R	GCTTCAGACAGGCGGCTTTA
	NF-κB-F	GCCTGACACCAGCATTTGA
	NF-κB-R	CAAACCAAACAGCCTCACG
	ACTIN-F	TCAGGTCATCACTATCGGCA
	ACTIN-R	GGCATAGAGGTCTTTACGGAT
MS-PCR	*p2x3r*-M-F1	GAATTTGGGATCGGTTTAGAGAGC
	p2x3r-M-R1	CGCGAAACGATTAAAATAAATCGAT
	p2x3r-U-F1	AATTTGGGATTGGTTTAGAGAGTGT
	p2x3r-U-R1	CCCCACAAAACAATTAAAATAAATCAAT
BS-PCR	*p2x3r*-F	GAGAGGAAGATTTGGTTAGAAA
	p2x3r-R	CTAAAAAACAAACACAATCACC
ChIP	*p2x3r*/NF-κB-67-F	CTTACATCTCAACCCGACACC
	p2x3r/NF-κB-304-R	GGGACGATTGGGATGGA
	p2x3r/NF-κB-247-F	AATGGATTCGCCCACTGC
	p2x3r/NF-κB-441-R	TTCCCCCGTATCCCTATCC
	p2x3r/NF-κB-425-F	ATAGGGATACGGGGGAAGG
	p2x3r/NF-κB-524-R	TCTTCCTCTCTATGGTTTGTGC
	p2x3r/NF-κB-503-F	GCACAAACCATAGAGAGGAAGA
	p2x3r/NF-κB-605-R	CCTCGCTTTAGACGACCAG
	p2x3r/NF-κB-581-F	GTGCCCCTGGTCGTCTAA
	p2x3r/NF-κB-689-R	CTTTGAAGAGCAGCCTGTAACT

as described previously (27,29). Specific primers were designed to amplify CpG-rich regions in the *p2x3r* promoter (Table 1).

Chromatin Immunoprecipitation Assays

A chromatin immunoprecipitation (ChIP) assay was performed using the Upstate Kit (EMD Millipore, Billerica, MA) according to the manufacturer's instructions, as described previously (9,30). Five NF-κB consensus site–specific primers in the *p2x3r* promoter are shown in Table 1.

Lentivirus Vector Generation and Intrathecal Injection

As described previously (31), the siRNA targeting the cDNA sequence of rat p65 (GenBank Accession #NM_199267) was used. The sequences of the siRNA were as follows: 5-GCAGUUCGAUGCUGAUGAAUU-3. An additional scrambled sequence was also designed as a negative control (NC). The replication-deficient, self-inactivating LV pFU-GW-RNAi-GFP (Shanghai Genechem Co., Ltd.) was generated. The cDNAs corresponding to the p65 siRNA and NC were subcloned into the vector pFU-GW-RNAi-GFP. The resulting recombinant LVs were designated as LV-p65 siRNA or LV-NC. The titer of lentivirus was determined by a hole-by-dilution titer assay. The final titer of LV-p65 siRNA and LV-NC was 1×10^9 transduction units (TU)/mL. To determine the level of efficiency of infection of virus constructs, a pilot study with LV-GFP was performed. The lentiviruses were then injected into rats intrathecally. Experiments were performed 4 weeks later.

Data Analysis

Data were expressed as the mean ± SEM. Software OriginPro 8 (OriginLab, Northampton, MA), MATLAB (MathWorks, Natick, MA), and SPSS version 17.0 were used for data analysis. Significance was determined using a two-sample *t* test, Mann-Whitney *U* test, Dunn post hoc test following Friedman ANOVA, two-way repeated-measures ANOVA followed by Tukey post hoc test, or χ^2 test, as appropriate. A P value <0.05 was considered to be statistically significant.

RESULTS

Attenuation of Mechanical Allodynia and Thermal Hyperalgesia by P2XR Antagonist in Diabetic Rats

Consistent with our previous studies (13,23), a single injection of STZ produced hindpaw allodynia in rats

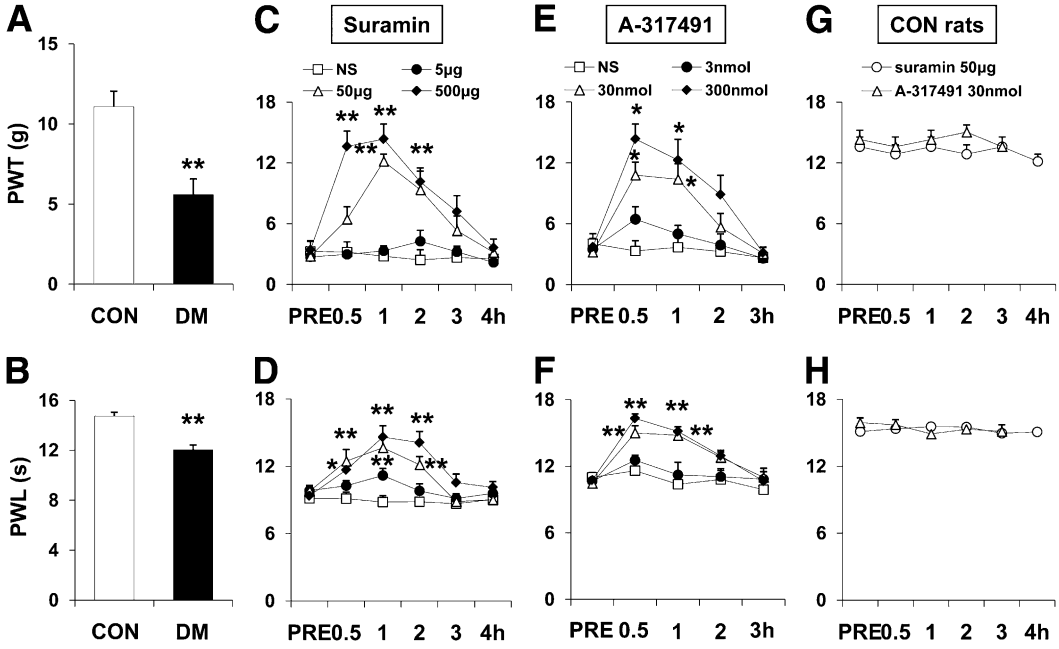

Figure 1—Treatment with purinergic receptor antagonist attenuates diabetic mechanical allodynia and thermal hyperalgesia. *A*: The mechanical PWT decreased substantially 4 weeks after STZ injection. The mechanical PWT was 11.07 ± 0.98 and 5.60 ± 0.97 g, respectively, for control (CON) rats and diabetic (DM) rats (n = 10 for each group, $^{**}P < 0.01$, compared with CON rats, Mann-Whitney *U* test). *B*: The mean PWL to radiant heat stimulation decreased 4 weeks after STZ injection. The thermal PWL was 14.74 ± 0.30 and 12.04 ± 0.38 s, respectively, for CON and DM rats (n = 10 for each group, $^{**}P < 0.01$, compared with CON rats, two-sample *t* test). *C*: Intrathecal injection of P2 receptor inhibitor suramin attenuated the PWT in a dose-dependent and time-dependent manner in diabetic rats (n = 6, 6, 6, and 6, respectively, for the NS, 5, 50, and 500 μg/kg groups; $^{**}P < 0.01$, compared with NS, Friedman ANOVA). *D*: A similar effect was found in PWL (n = 6, 6, 6, and 6, respectively, for the NS, 5, 50, and 500 μg/kg groups; $^{*}P < 0.05$, $^{**}P < 0.01$, compared with NS, two-way repeated-measures ANOVA followed by Tukey post hoc test). *E*: Intrathecal injection of a potent P2X3R and P2X2R/P2X3R inhibitor, A-317491, also attenuated the PWT in a dose-dependent and time-dependent manner in diabetic rats (n = 6, 6, 6, and 6, respectively, for the NS, 3, 30, and 300 nmol/kg groups; $^{*}P < 0.05$, compared with the NS group, Friedman ANOVA). *F*: A similar effect was found in PWL (n = 6, 6, 6, and 6, respectively, for the NS, 3, 30, and 300 nmol/kg groups; $^{**}P < 0.01$, compared with the NS group, two-way repeated-measures ANOVA followed by Tukey post hoc test). *G* and *H*: Suramin at a dose of 50 μg/kg and A-317491 at a dose of 30 nmol/kg did not produce any effect on PWT and PWL in CON rats (n = 6 for each group). PRE, before.

(Fig. 1*A*, n = 10 rats for each group, $^{**}P < 0.01$ compared with control rats, Mann-Whitney *U* test; Fig. 1*B*, n = 10 rats for each group, $^{**}P < 0.01$, compared with control rats, two-sample *t* test). Intrathecal injection of suramin, a nonselective P2 receptor antagonist, attenuated the PWT in a dose-dependent and time-dependent manner in diabetic rats (Fig. 1*C*, n = 6 rats for each group, $^{**}P < 0.01$, compared with NS, Friedman ANOVA). A similar effect was found in PWL (Fig. 1*D*, n = 6 rats for each group, $^{*}P < 0.05$, $^{**}P < 0.01$, compared with NS, two-way repeated-measures ANOVA followed by Tukey post hoc test). The maximal inhibitory effects for suramin were observed at a dose of 500 μg/kg. Intrathecal injection of A-317491, a potent antagonist for P2X3Rs and P2X2Rs/P2X3Rs, significantly attenuated the PWT (Fig. 1*E*, n = 6 rats for each group, $^{*}P < 0.05$, compared with NS, Friedman ANOVA) and PWL (Fig. 1*F*, n = 6 rats for each group, $^{**}P < 0.01$, compared with NS, two-way repeated-measures ANOVA followed by Tukey post hoc test) in diabetic rats. The maximal inhibitory effects were observed at a dose of 300 nmol/kg for A-317491. Of note is that suramin at a dose of 50 μg/kg or A-317491 at a dose of 300 nmol/kg did not produce any effect on PWT and PWL in healthy control rats (Fig. 1*G* and *H*, n = 6 rats for each group).

Increase in Function and Expression of P2X3Rs of Diabetic Rats

To test the hypothesis that ATP signaling is enhanced in diabetic rats, currents evoked by ATP in acutely isolated DRG neurons were measured using whole-cell patch-clamp recording techniques. Hindpaw-innervating DRG neurons were labeled by the fluorescent dye DiI (Fig. 2*A*, top, arrow). At a holding potential of −60 mV, ATP (20 μmol/L) evoked the following two types of inward currents, as described previously (19): fast inactivating currents and slow inactivating currents. Since the slow inactivating currents was evoked in <10% of neurons and this figure did not change in STZ-induced diabetes, only the fast inactivating currents were included in the current study (Fig. 2*B*, top). The average peak current density obtained from diabetic rats was significantly increased (Fig. 2*B*, bottom, n = 11 cells for each group, $^{**}P <$ 0.01 compared with control rats, two-sample *t* test). In

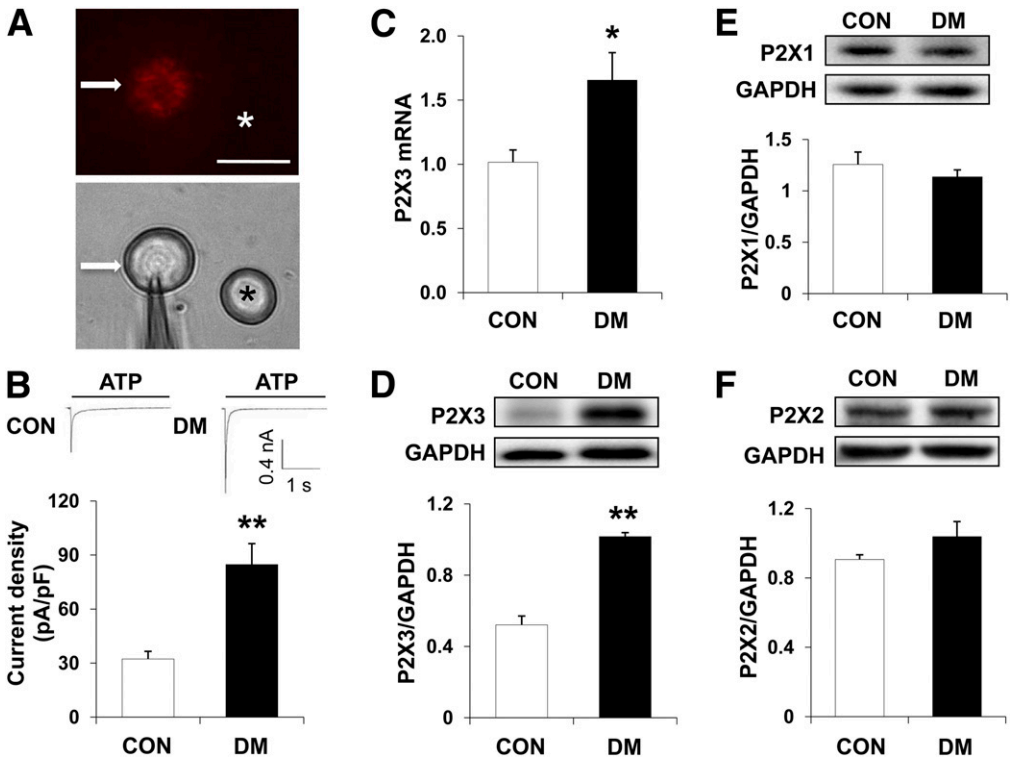

Figure 2—Induction of diabetes with STZ sensitizes P2X3Rs in DRG neurons. *A*, Top: An example of a DiI-labeled DRG neuron (arrow) innervating the hindpaw. The asterisk indicates the place where a neuron is not labeled by DiI. Bottom: Phase image of the same DRG neuron labeled by DiI is shown on the left (arrow), and the neuron not labeled by DiI is shown on the right (*). Scale bar = 50 μm. Patch-clamp recordings were performed on DiI-labeled hindpaw neurons. *B*, Top: An example of ATP-evoked inward currents in DiI-labeled neurons under voltage-clamp conditions. Bottom: Bar graph showing an average of ATP-induced current density of DiI-labeled DRG neurons from control (CON) and diabetic (DM) rats. The average peak current density values obtained from CON and DM rats were 32.28 ± 4.23 and 84.75 ± 11.59 pA/pF, respectively, in DiI-labeled DRG neurons (n = 11 cells for each group, $^{**}P < 0.01$, compared with the CON group, two-sample t test). *C*: RT-PCR assays demonstrated a significant upregulation of P2X3R mRNA expression in L4–L6 DRGs in DM rats compared with age- and sex-matched CONs (n = 4 for each group, $^{*}P < 0.05$, compared with CON rats, two-sample t test). *D*: P2X3R protein expression was greatly enhanced in L4–L6 in diabetic rats (n = 4 for each group, $^{**}P < 0.01$, compared with CON rats, two-sample t test). *E* and *F*: P2X1R and P2X2R protein expression were not significantly altered in diabetic rats when compared with age- and sex-matched CONs (n = 6 for CON group, n = 3 for DM group, $P > 0.05$, compared with CON rats, two-sample t test).

addition, the expression of both P2X3R mRNA and proteins was significantly higher in diabetes than in control rats (Fig. 2*C* and *D*, n = 4 rats for each group, $^{*}P < 0.05$, $^{**}P < 0.01$, compared with control rats, two-sample t test). In contrast, the expression of P2X1 and P2X2 receptors was not significantly altered 4 weeks after STZ injection (Fig. 2*E* and *F*, n = 6 for control rats, n = 3 for diabetic rats).

Demethylation of CpG Sites of *p2x3r* Gene Promoter Region and Downregulation of DNA Methyltransferases in Diabetic Rats

To determine whether an epigenetic mechanism contributes to the upregulation of P2X3R expression, DNA methylation status at the promoter region of the *p2x3r* gene was examined with MSP and a bisulfite genomic sequence assay. The genomic structure of rat *p2x3r* gene contains one CpG island in the promoter region (Fig. 3*A*). When the frequency of CpG is high in certain sections of the genome, these segments are known as CpG islands. Methylation occurs only in the CpG dinucleotide sites. All samples yielded methylated and unmethylated bands from control and diabetic rats, as determined by MSP assay (Fig. 3*B*). The ratio of methylated to unmethylated CpG sites was greatly reduced (Fig. 3*B*, n = 8 for each group, $^{*}P < 0.05$, compared with control rats, two-sample t test). To further confirm the methylation status of CpG sites within the *p2x3r* promoter, DNA sequencing was performed on PCR products of the 406-bp fragment (−1,737 to −1,332) obtained after the treatment of genomic DNA samples with sodium bisulfite. As shown in Fig. 3*A*, the 406-bp fragment contains 18 CpG sites. All DRG samples from control and diabetic rats were successfully sequenced (Fig. 3*C*). The degree of methylation of the CpG sites within the fragment was significantly reduced in DRGs 4 weeks after the induction of diabetes (Fig. 3*D*, n = 4 for each group, $^{*}P < 0.05$, compared with control rats, χ^2 test), which is consistent with the results of the MSP assay. In addition, the expression level of DNA methyltransferase (DNMT) 3b was remarkably reduced, while the expression level of DNMT3a was not altered in diabetic rats (Fig. 3*E*,

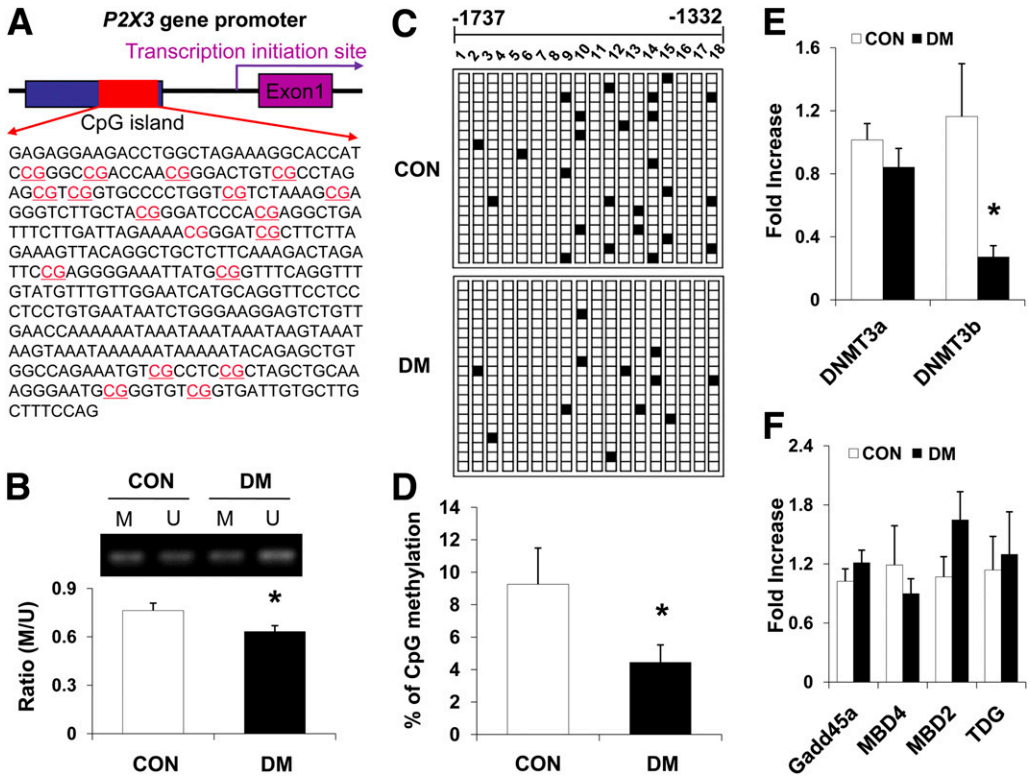

Figure 3—The induction of diabetes by STZ results in the demethylation of CpG sites of the *p2x3r* gene promoter region and the down-regulation of DNMTs. *A*: Schematic of a CpG island showing the locations of the 18 CpG sites (in red and underlined) in the *p2x3r* gene promoter area. *B*: Representative PCR results of the *p2x3r* promoter region using one pair of primers for methylation-specific and unmethylation–specific amplifications of genomic DNA from DRG samples prepared from control (CON) rats and diabetic (DM) rats. PCR products cover regions of MSP primer. Bar graph below the gel images shows ratios of methylated (M) to unmethylated (U) products. STZ-induced diabetes significantly reduced the the M/U ratio of CpG sites (n = 8 for each group, $^*P < 0.05$, compared with CON rats, two-sample t test). *C*: Each square indicates the clones from CON rats (top) and DM rats (bottom). Twenty clones were subjected to bisulfite sequencing. The methylated clones for an individual CpG site are labeled in black. *D*: STZ-induced diabetes significantly reduced the percentage of methylated CpG sites (n = 4 for each group, $^*P < 0.05$, compared with CON rats, χ^2 test). *E*: STZ-induced diabetes leads to a reduced expression of DNMT3b in DRG samples when compared with CON rats (n = 4 for each group, $^*P < 0.05$, two-sample t test), while the expression of DNMT3a was not altered (n = 4 for each group, $P > 0.05$, compared with CON rats, two-sample t test). *F*: STZ-induced diabetes did not produce significant changes in the expression of growth arrest and of Gadd45a, MBD2, MBD4, and TDG in DRG samples when compared with CON rats (n = 4 for each group, $P > 0.05$, compared with CON rats, two-sample t test).

n = 4 for each group, $^*P < 0.05$, compared with control rats, two-sample t test). We also examined the expression of growth arrest and DNA damage–inducible protein α (Gadd45a), methyl-binding domain protein (MBD) 2, MBD4, and thymine DNA glycosylase (TDG) of L4–L6 DRGs in control and diabetic rats. None of these molecules was altered in their expression in diabetic rats (Fig. 3*F*, n = 4 for each group).

Promotion of Binding Ability of p65 With *p2x3r* Gene Promoter

We next determined whether NF-κB signaling was involved in P2X3R expression. The p65 antibody used in the study detects the total expression of p65, including phosphorylated and total proteins, and it was not a phosphorylation-independent antibody. p65 was coexpressed in P2X3Rs-positive hindpaw-innervating DRG neurons (Fig. 4*A*). As indicated in Fig. 4*B*, five transcription-binding sites for p65 were found in the *p2x3r* gene promoter (http://www.gene-regulation.com/pub/programs/alibaba2/index.html). The ChIP assay demonstrated a dramatic increase in p65 binding activities to the *p2x3r* promoter region for p65 binding site 1 (Fig. 4*C*, n = 4 for each group, $^*P < 0.05$, compared with control rats, two-sample t test). p65 binding sites 4 (Fig. 4*D*, n = 4 for each group) and 5 (Fig. 4*E*, n = 4 for each group) in diabetic rats were not remarkably altered when compared with age- and sex-matched control rats. The predicted p65 binding sites 2 and 3 were not confirmed by the ChIP assay in this study (data not shown). Nevertheless, these data indicated an increase in the interaction between p65 and the *p2x3r* promoter region in STZ-induced diabetes.

Suppression of Mechanical Allodynia and Thermal Hyperalgesia and P2X3R Expression by PDTC Treatment

To determine whether NF-κB plays a role in the development of diabetic pain hypersensitivity, we examined the

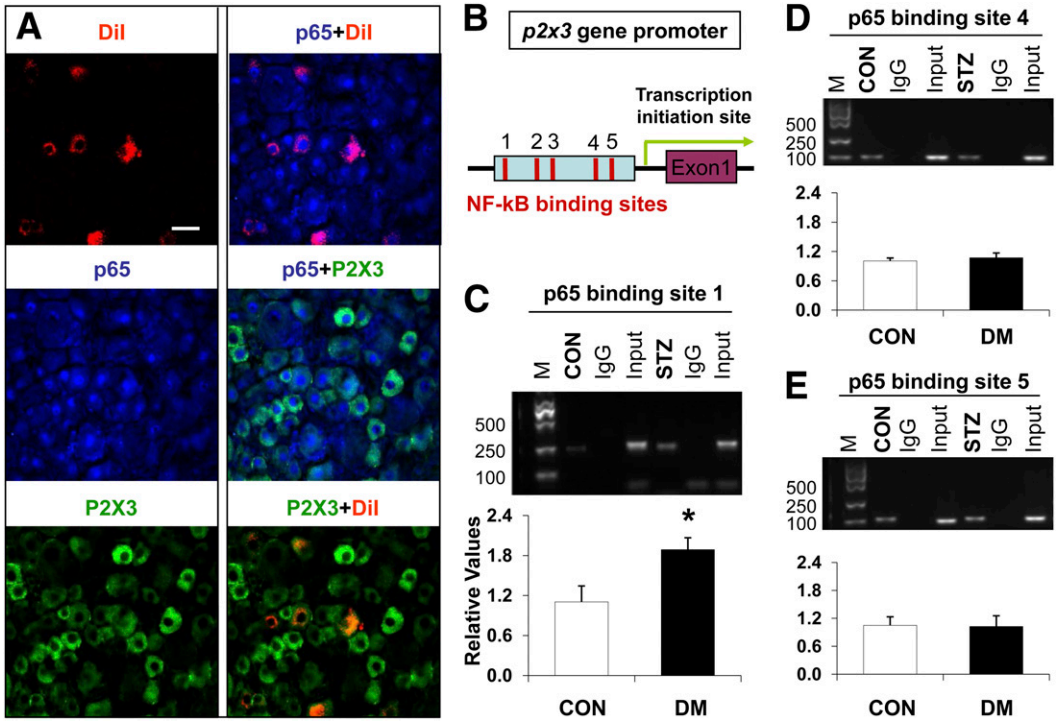

Figure 4—STZ-induced diabetes promotes binding ability of p65 with *p2x3r* gene promoter. *A*: Hindpaw-innervated L5 DRG neurons were labeled with DiI (red, top left) injected into the plantar skin of bilateral hindpaws. p65-positive cells are shown in blue (middle left). P2X3R-positive cells were shown in green (bottom left). Merge of double labeling of DiI and p65 (top right). Merge of p65-positive staining and P2X3R labeling (middle right). Merge of P2X3R-positive staining and DiI labeling (bottom right). Scale bar = 50 μm. *B*: Schematic of *p2x3r* gene promoter showing locations of the five binding sites for NF-κB in the CpG island. *C*: Potentiated interaction between p65 and *p2x3r* promoter regions. A specific anti-p65 antibody or normal mouse IgG was used for immunoprecipitation. ChIP assay findings indicated a significant increase in the binding activity of p65 with the first binding site of the promoter of the *p2x3r* gene in diabetic (DM) rats compared with age-matched control (CON) rats ($n = 4$ for each group, $^*P < 0.05$, compared with CON rats, two-sample *t* test). *D* and *E*: ChIP assays indicated no significant change in the binding activity of p65 with the fourth and fifth binding sites of the promoter of the *p2x3r* gene in DM rats compared with age-matched CON rats ($n = 4$ for each group, $P > 0.05$, compared with CON rats, two-sample *t* test). The binding activity of p65 with the second and third binding sites of the promoter of *p2x3r* gene was not observed in CON and DM rats. M, methylated.

expression of p65 in L4–L6 DRGs in STZ-induced diabetes. The expression of p65 both at the protein level (Fig. 5*A*, $n = 3$ for control rats, $n = 4$ for diabetic rats, $^*P < 0.05$, compared with control rats, two-sample *t* test) and the mRNA level (Fig. 5*B*, $n = 4$ for control rats, $n = 8$ for diabetic rats, $^*P < 0.05$, compared with control rats, two-sample *t* test) was significantly enhanced in L4–L6 DRGs 4 weeks after STZ injection when compared with age- and sex-matched control rats. Intraperitoneal injection of PDTC (50 mg/kg, once daily for 7 consecutive days starting 3 weeks after the STZ injection) greatly attenuated the PWT and PWL (Fig. 5*C* and *D*, $n = 8$ rats for each group, $^{**}P < 0.01$, compared with the NS group, two-sample *t* test). PDTC (50 mg/kg) did not produce any effect on PWT and PWL in control rats (Fig. 5*E* and *F*, $n = 5$ for each group). PDTC treatment also markedly suppressed P2X3R expression at the protein level (Fig. 5*G*, $n = 6$ rats for each group, $^{**}P < 0.01$, compared with the NS group, two-sample *t* test) and mRNA level in diabetic rats (Fig. 5*H*, $n = 6$ rats for NS, $n = 3$ rats for PDTC, $^*P < 0.05$, compared with the NS group, Mann-Whitney *U* test). The results suggested that p65 plays a role in diabetic pain hypersensitivity through the regulation of P2X3R expression.

Suppression of P2X3R Activities and Diabetic Mechanical Allodynia and Thermal Hyperalgesia by Silencing p65 Expression by LV-Derived siRNA

To further confirm the role of p65 signaling in diabetic pain hypersensitivity, we applied p65 siRNA to specifically knock down p65 expression. We first developed a highly efficient method of lentivirus-mediated delivery of siRNA targeting of p65 for gene silencing, as described previously (31). This method successfully transduced LV-GFP into cultured DRG neurons in vitro (data not shown) and in vivo by a single intrathecal injection. As shown in Fig. 6, hindpaw-innervating L5 DRG neurons were labeled by DiI (Fig. 6*A* and *D*, red, arrows). Green signals indicated that the LV-GFP-NC siRNA (Fig. 6*B*) or LV-GFP-p65 siRNA (Fig. 6*E*) was successfully transduced into these neurons, respectively. P2X3R-positive neurons were labeled in blue in Fig. 6*C* and *F*. The arrows in Fig. 6*B* and *E* indicate that these neurons were DiI and GFP

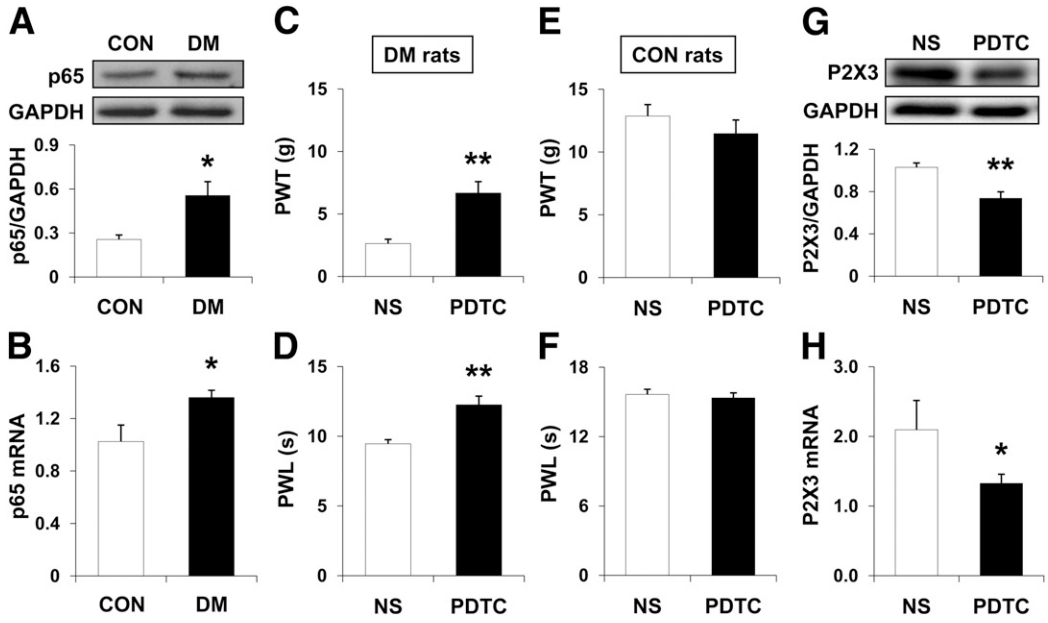

Figure 5—Treatment with the p65 inhibitor PDTC reverses the upregulation of P2X3Rs and attenuates diabetic (DM) mechanical allodynia and thermal hyperalgesia. *A*: p65 protein expression was greatly enhanced in L4–L6 DRGs in DM rats compared with age-matched and sex-matched control (CON) rats (n = 3 for the CON group, n = 4 for the DM group, $^*P < 0.05$, compared with CON rats, two-sample t test). *B*: RT-PCR assays demonstrated a significant upregulation of p65 mRNA expression in L4–L6 DRGs in DM rats (n = 4 for CON group, n = 8 for DM group, $^*P < 0.05$, compared with CON rats, two-sample t test). *C* and *D*: Intraperitoneal injection of PDTC (at a dose of 50 mg/kg) or the same volume of NS once daily for 7 consecutive days increased PWT and PWL in STZ-injected rats (n = 8 for each group, $^{**}P < 0.01$, compared with NS, two-sample t test). *E* and *F*: PDTC at a dose of 50 mg/kg did not produce any effect on PWT and PWL in CON rats (n = 5 for each group). *G*: Administration of PDTC (50 mg/kg once daily for 7 consecutive days) dramatically reduced P2X3R expression at the protein level (n = 6 for the each group, $^{**}P < 0.01$, compared with the NS group, two-sample t test). *H*: Administration of PDTC (at a dose of 50 mg/kg, once daily for 7 consecutive days) significantly reduced the expression of P2X3R mRNA (n = 6 for the NS group, n = 3 for the PDTC group, $^*P < 0.05$, compared with NS, Mann-Whitney U test).

double positive. The empty arrowheads in Fig. 6*F* indicated that these neurons were DiI and GFP double positive, but P2X3R negative.

After intrathecal injection of LV-p65 siRNA (1×10^7 TU) in diabetic rats, the percentage of P2X3R-positive neurons in DiI-labeled neurons was significantly decreased (Fig. 6*G*, n = 4 for the each group, $^{**}P < 0.01$, compared with NC siRNA, two-sample t test). The expression of p65 was also remarkably decreased in L4–L6 DRGs (Fig. 6*H*, n = 4 for each group, $^*P < 0.05$, compared with NC siRNA, two-sample t test). Importantly, the delivery of siRNA targeting p65 for gene silencing also decreased the expression of P2X3Rs (Fig. 6*I*, n = 4 for each group, $^*P < 0.05$, compared with NC siRNA, two-sample t test).

In addition, LV-p65 siRNA treatment markedly suppressed the current evoked by ATP in diabetic rats (Fig. 7*A* and *B*, n = 12 cells for NC siRNA, n = 11 cells for p65 siRNA, $^{**}P < 0.01$, compared with NC siRNA, two-sample t test). The delivery of siRNA targeting p65 significantly attenuated mechanical allodynia (Fig. 7*C*, n = 8 for each group, $^{**}P < 0.01$, compared with NC siRNA, Friedman ANOVA) and thermal hyperalgesia (Fig. 7*D*, n = 8 for each group, $^{**}P < 0.01$, compared with NC siR group, Friedman ANOVA). However, LV-p65 siRNA did not produce any effect on PWT and PWL in control rats (Fig. 7*E* and *F*, n = 5 rats for each group). These results further suggested that p65 might regulate the function of P2X3Rs through regulating its expression, thus contributing to diabetic pain hypersensitivity.

Suppression of Mechanical Allodynia and Thermal Hyperalgesia, and the Expression of p65 and P2X3Rs of Diabetic Rats by Insulin Treatment

We next determined whether insulin treatment attenuated mechanical allodynia and thermal hyperalgesia and reversed changes in the expression of p65 and P2X3Rs in diabetic rats. Starting on day 8 after STZ injection, each rat was given two daily subcutaneous injections of either 1–4 units of insulin (human recombinant insulin; Novo Nordisk) in 0.2 mL or the same volume of NS as a control for 21 days. The insulin dose was adjusted to correct hyperglycemia and to avoid hypoglycemia as well (32). The average blood glucose level was significantly decreased 1 week later and was maintained at a relative low level for another 2 weeks within our observation period of time, and the body weight of insulin-treated rats exhibited a steady increase (Supplementary Table 2; n = 7 for each group, $^{**}P < 0.01$, compared with NS, two-way repeated-measures ANOVA followed by Tukey post hoc test). In addition, insulin treatment reversed PWT and

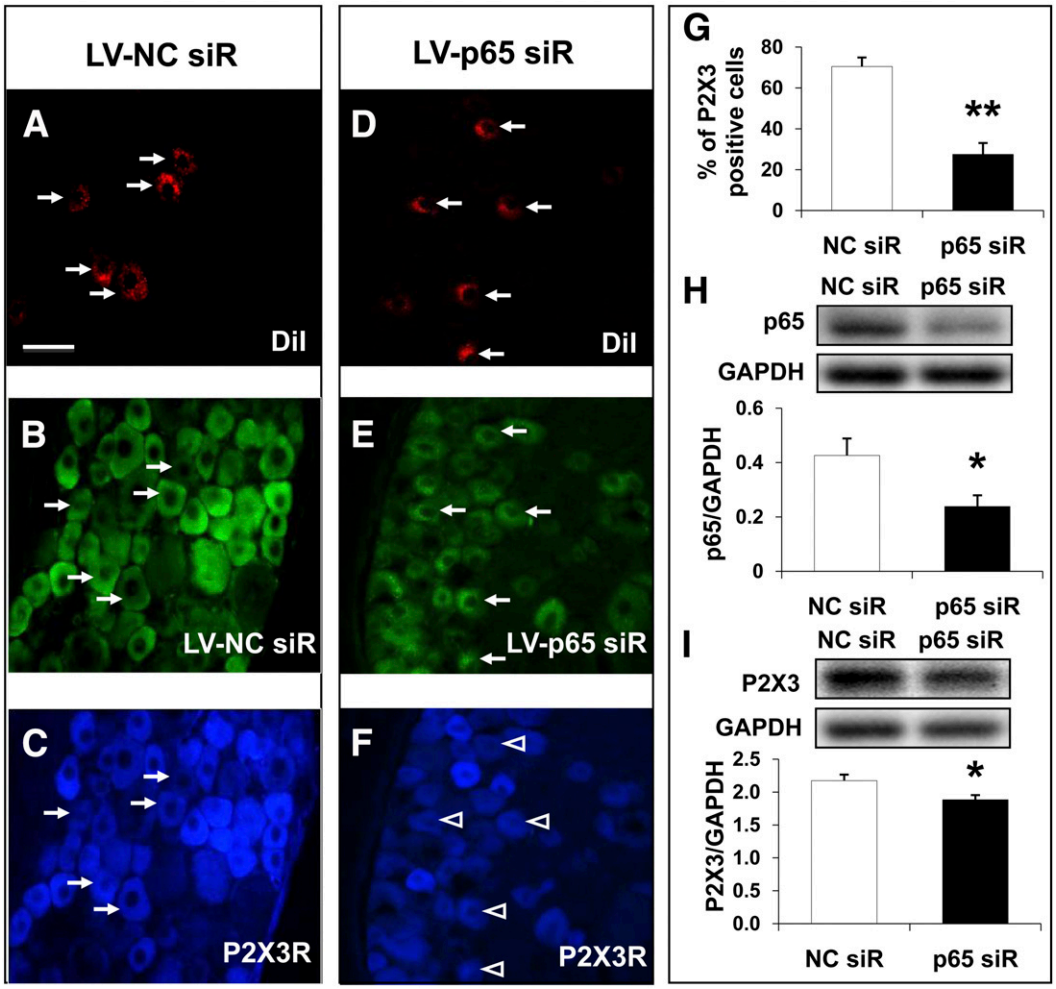

Figure 6—Silencing p65 expression by LV-derived siRNA (siR) reduces the expression of P2X3Rs. NC siRNA (NC siR) was used as a control (CON). The left column shows that LV-NC siRNA did not change the fluorescence intensity of P2X3Rs. *A*: Neurons in red (arrows) are DiI-labeled L5 DRG neurons innervating the hindpaw. *B*: Neurons in green (arrows) are LV-GFP-NC siRNA-transduced neurons 4 weeks after intrathecal injection. *C*: Neurons in blue (arrows) are P2X3R-positive DRG neurons. The middle column showed that LV-p65 siRNA reduces the fluorescence intensity of P2X3Rs. More LV-p65 siRNA transfection into neurons (shown as a strong green fluorescence) results in less expression of P2X3Rs (shown as a weak blue fluorescence). *D*: Neurons in red (arrows) are DiI-labeled L5 DRG neurons innervating the hindpaw. *E*: Neurons in green are LV-GFP-p65 siRNA-transduced neurons 4 weeks after intrathecal injection. *F*: Neurons in blue are P2X3R-positive DRG neurons. It is of note that GFP-positive neurons (indicated by arrows in *E*) are negative or weakly stained with P2X3R antibodies (indicated by arrowheads in *F*). Scale bar = 50 μm. *G*: The percentage of P2X3R– and DiI–double-positive neurons among the total of DiI-labeled DRG neurons was dramatically reduced after the transfection of LV-GFP-p65 siRNA ($n = 4$ for the each group, $^{**}P < 0.01$, compared with the NC siR group, two-sample *t* test). *H*: The delivery of siRNA targeting p65 at 1×10^7 TU for gene silencing significantly decreased the expression of p65 in L4–L6 DRGs in diabetic rats ($n = 4$ for each group, $^{*}P < 0.05$, compared with the NC siR group, two-sample *t* test). *I*: The expression of P2X3Rs was significantly decreased after intrathecal injection of LV-GFP-p65 siRNA at 1×10^7 TU in diabetic rats ($n = 4$ for each group, $^{*}P < 0.05$, compared with the NC siR group, two-sample *t* test).

PWL when compared with NS (Fig. 8*A* and *B*, $n = 7$ for each group, $^{*}P < 0.05$, $^{**}P < 0.01$, compared with NS, Friedman ANOVA). This inhibitory effect was exhibited from 1 to 3 weeks after insulin treatment. More importantly, insulin treatment significantly downregulated the expressions of p65 and P2X3Rs in L4–L6 DRGs in diabetic rats (Fig. 8*C* and *D*, $n = 4$ for each group, $^{*}P < 0.05$, $^{**}P < 0.01$, compared with NS, two-sample *t* test). These data suggest that insulin loss or/and hyperglycemia but not STZ neuronal toxicity (33) are most likely the causes for many of the biochemical disorders observed in the current study.

DISCUSSION

We demonstrated that P2X3Rs play an important role in the development of peripheral diabetic neuropathic pain. In our previous study (13), we have reported the role of P2X3Rs in diabetic allodynia 2 weeks after STZ injection. In the current study, we further extended our observation time period to 4 weeks after STZ injection since STZ-induced mechanical allodynia and thermal hyperalgesia were attenuated by a nonselective P2 receptor inhibitor suramin and by a potent P2X3R and P2X2R/P2X3R antagonist, A-317491. In addition, we showed that P2X3R

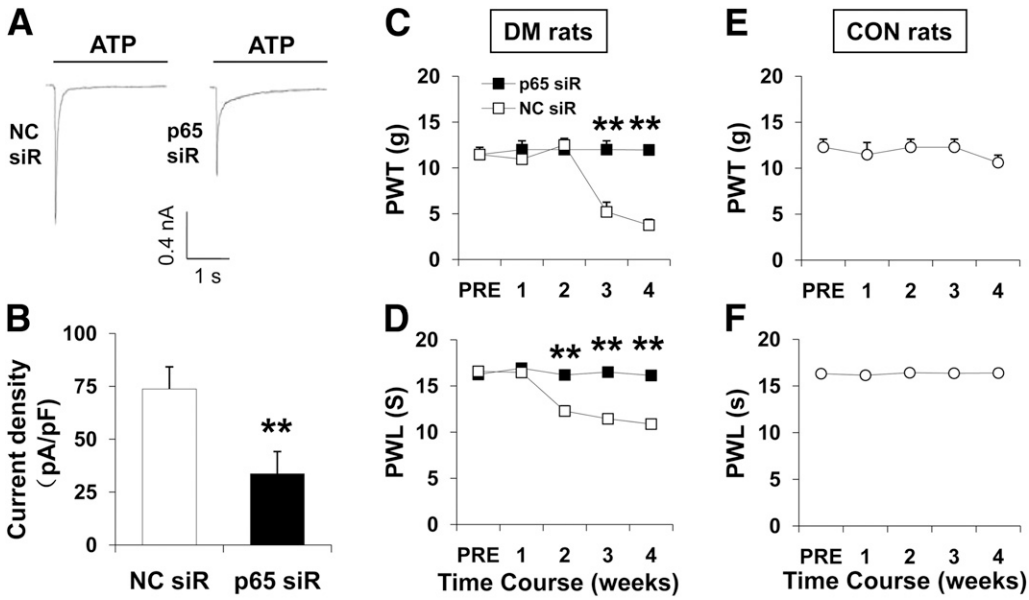

Figure 7—Silencing p65 expression by LV-derived siRNA suppresses P2X3R activities and attenuates diabetic (DM) mechanical allodynia and thermal hyperalgesia. *A*: An example of ATP-evoked inward current traces recorded from LV-p65 siRNA (p65 siR)–injected and NC siRNA (NC siR)–injected rats with diabetes. *B*: Bar graph shows a drastic reduction in ATP-evoked current density after LV-p65 siR injection (n = 12 cells for the NC siR group, n = 11 cells for the p65 siR group, $^{**}P < 0.01$, compared with the NC siR group, two-sample t test). *C*: Delivery of siRNA targeting p65 reversed PWT when compared with the NC siR group (n = 8 for each group, $^{**}P < 0.01$, compared with the NC siR group, Friedman ANOVA). This inhibitory effect was exhibited from 3 to 4 weeks after STZ injection within our observation time period. *D*: Delivery of siRNA targeting p65 reversed PWL when compared with NC siR (n = 8 for each group, $^{**}P < 0.01$, compared with the NC siR group, Friedman ANOVA). This inhibitory effect was exhibited from 2 to 4 weeks after STZ injection. *E*: Delivery of siRNA targeting p65 did not produce any effect on PWT in healthy control (CON) rats (n = 5 for each group). *F*: Delivery of siRNA targeting p65 did not produce any effect on PWL in healthy CON rats (n = 5 for each group). PRE, before.

function was greatly enhanced, which was likely mediated by the upregulation of P2X3R expression 4 weeks after STZ induction of diabetes. This result is different from our previous report that membrane P2X3R protein expression was significantly upregulated without alteration in the expression of total P2X3R proteins in rat DRGs 2 weeks after STZ injection (13). Although the detailed mechanisms are unknown, these results suggest that mechanisms underlying the potentiation of ATP-induced responses are different with the progress of the diabetes. At the beginning of diabetes (i.e., 2 weeks), the enhanced ATP-induced responses might be due to the promoted trafficking of P2X3Rs from cytoplasm to cell membrane (13). With the development of diabetic mechanical allodynia and thermal hyperalgesia (i.e., 4 weeks), the upregulation of P2X3R expression might be a major contributor to the potentiation of ATP-induced responses. However, the upregulation is gene specific since the expression of P2X1R and P2X2R was not significantly altered in this setting. Therefore, it is most likely the case that the *p2x3r* gene might be an effective facilitator of STZ-induced diabetic pain hypersensitivity. Once activated, P2X3Rs cause pain, most likely because of increased drive from the periphery, increased spontaneous activity of DRG neurons, and/or increased sensitivity in the dorsal horn of the spinal cord (34,35).

The most important finding is that *p2x3r* gene was significantly demethylated in diabetic rats. Emerging evidence (36,37) shows that epigenetic regulations (i.e., aberrant DNA methylation and histone acetylation) are involved in gene expression. Gene promoter DNA methylation suppresses gene expression, whereas gene promoter DNA demethylation facilitates gene upregulation (38,39). Wang et al. (40) reported a role of DNA methylation in nerve injury–induced pain. We have previously reported that DNA demethylation of the *cbs* gene promoter is involved in inflammatory hyperalgesia (27) and gastric hypersensitivity (9), which is consistent with the upregulation of cystathionine β-synthetase (an endogenous synthetase of hydrogen sulfide) and mRNA. Methylation occurs only in the CpG dinucleotide sites (41,42). The increase in demethylation of the *p2x3r* promoter region would give rise to an upregulation of P2X3R expression in diabetic rats. To date, the mechanism of DNA methylation remains largely unknown. In mammals, there are four types of DNMTs in regulating methylation status (38). DNMT3a and DNMT3b, two major enzymes for de novo methyltransferase, are mainly responsible for the methylation of CpG islands (43,44). The reduction of the methylase (i.e., DNMT3b) can lead to the demethylation state, although the expression of demethylation enzymes such as TDG, MBD2, MBD4, and Gadd45a was

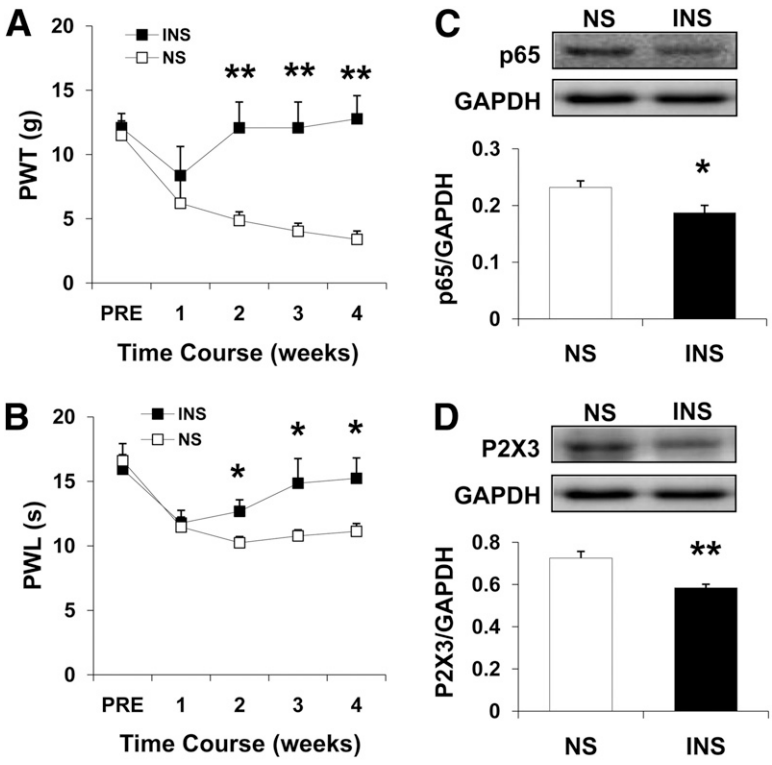

Figure 8—Insulin treatment attenuates diabetic mechanical allodynia and thermal hyperalgesia and downregulates the expressions of p65 and P2X3 receptors. Starting on day 8 after STZ injection, each rat was given two daily subcutaneous injections of either 1–4 units of insulin (human recombinant insulin; Novo Nordisk) in 0.2 mL or the same volume of NS as control (CON) rats for 21 days. *A*: Insulin (INS) treatment reversed PWT when compared with NS treatment ($n = 7$ for each group, $^{**}P < 0.01$, compared with NS group, Friedman ANOVA). This inhibitory effect was exhibited from 1 to 3 weeks after insulin injection within our observation time period. *B*: INS treatment reversed PWL when compared with NS treatment ($n = 7$ for each group, $^{*}P < 0.05$, compared with the NS group, Friedman ANOVA). This inhibitory effect was exhibited from 1 to 3 weeks after insulin injection. *C*: INS treatment significantly decreased the expression of p65 in L4–L6 DRGs in diabetic rats ($n = 4$ for each group, $^{*}P < 0.05$, compared with NS group, two-sample *t* test). *D*: The expression of P2X3Rs was significantly decreased after INS treatment in diabetic rats ($n = 4$ for each group, $^{**}P < 0.01$, compared with the NS group, two-sample *t* test).

not significantly affected in STZ-induced diabetes. This is consistent with our previous report (9) that DNMT3a and DNMT3b were drastically downregulated in gastric DRGs under diabetic pain hypersensitivity conditions. This is, however, different from the finding in our previously published study (27) that an active mechanism is involved in inflammatory pain. Although the detailed mechanisms for this difference are unknown, it is most likely that the mechanism of diabetes-induced DNA demethylation is different from that of inflammation-induced DNA methylation but may share a common mechanism for neuropathic pain.

Demethylation of a gene promoter region leads to the exposure of a transcription factor binding site, thus allowing the transcription factor to bind. p65 plays an important role in inflammatory diseases, immune responses, and cell death by binding to the promoter region of various genes such as tumor necrosis factor-α (TNF-α), interleukin-1β, cyclooxygenase-2, and inducible nitric oxide synthase (45,46). We demonstrated that diabetes promoted the binding ability of p65 with demethylation of the *p2x3r* gene. In the development of diabetic neuropathy, p65 is the central link of multiple pathways. It can be activated by reactive oxygen species, advanced glycation end products, and other cytokines such as TNF-α (47,48). The activation of NF-κB can upregulate P2X3R expression and promote the production of cytokines such as TNF-α (45,46), thus forming a positive feedback loop to maintain the diabetic pain hypersensitivity. Of note is that Berti-Mattera et al. (49) showed a reduction in p65 in nuclear fractions of DRG in diabetic rats. Although the reasons for the difference are not clear, the disease duration (3 months vs. 4 weeks), the animal species (Lewis rats vs. SD rats), and the dosage of STZ used (60 vs. 65 mg/kg body wt) could be the causes. Since insulin treatment significantly attenuated the pain hypersensitivity in an association with the reduced expression of p65 and P2X3Rs, it is likely that insulin loss and/or hyperglycemia might be the triggers of gene expression. Future studies need to investigate the mechanisms in detail and the possible role of NF-κB p50 subunits in p65-mediated gene expression.

In conclusion, our findings demonstrated for the first time, to the best of our knowledge, that the upregulation of P2X3R expression is attributed to *p2x3r* gene promoter DNA demethylation and p65 activation. The enhanced

interaction of p65 with the *p2x3r* gene promoter would contribute to abnormal diabetic peripheral neuropathic pain. The results may provide promising clues for the development of new therapeutic strategies for managing intractable neuropathic pain in patients with diabetes.

Funding. This work was supported by grants from National Natural Science Foundation of China (31400947 to H.-H.Z., 81471041 to J.H., 31271258 to X.J., and 81230024 and 81471137 to G.-Y.X.) and from the Priority Academic Program Development of Jiangsu Higher Education Institutions of China.

Duality of Interest. No potential conflicts of interest relevant to this article were reported.

Author Contributions. H.-H.Z. and J.H. researched and analyzed the data and wrote the article. Y.-L.Z. researched and analyzed the data. X.Q., Z.-Y.S., P.-P.Y., and S.H. researched the data. X.J. contributed to the discussion and reviewed and edited the article. G.-Y.X. designed and supervised the experiments and edited the article. G.-Y.X. is the guarantor of this work and, as such, had full access to all the data in the study and takes responsibility for the integrity of the data and the accuracy of the data analysis.

References

1. Gooch C, Podwall D. The diabetic neuropathies. Neurologist 2004;10:311–322
2. Russell JW, Zilliox LA. Diabetic neuropathies. Continuum (Minneap Minn) 2014;20:1226–1240
3. Abbott CA, Malik RA, van Ross ER, Kulkarni J, Boulton AJ. Prevalence and characteristics of painful diabetic neuropathy in a large community-based diabetic population in the U.K. Diabetes Care 2011;34:2220–2224
4. Peltier A, Goutman SA, Callaghan BC. Painful diabetic neuropathy. BMJ 2014;348:g1799
5. Ziegler D. Treatment of diabetic polyneuropathy: update 2006. Ann N Y Acad Sci 2006;1084:250–266
6. Zilliox L, Russell JW. Treatment of diabetic sensory polyneuropathy. Curr Treat Options Neurol 2011;13:143–159
7. Chattopadhyay M, Mata M, Fink DJ. Continuous delta-opioid receptor activation reduces neuronal voltage-gated sodium channel (NaV1.7) levels through activation of protein kinase C in painful diabetic neuropathy. J Neurosci 2008;28:6652–6658
8. Grabauskas G, Heldsinger A, Wu X, Xu D, Zhou S, Owyang C. Diabetic visceral hypersensitivity is associated with activation of mitogen-activated kinase in rat dorsal root ganglia. Diabetes 2011;60:1743–1751
9. Zhang HH, Hu J, Zhou YL, et al. Promoted interaction of nuclear factor-κB with demethylated cystathionine-β-synthetase gene contributes to gastric hypersensitivity in diabetic rats. J Neurosci 2013;33:9028–9038
10. Huang Y, Zang Y, Zhou L, Gui W, Liu X, Zhong Y. The role of TNF-alpha/NF-kappa B pathway on the up-regulation of voltage-gated sodium channel Nav1.7 in DRG neurons of rats with diabetic neuropathy. Neurochem Int 2014;75:112–119
11. Pabbidi RM, Yu SQ, Peng S, Khardori R, Pauza ME, Premkumar LS. Influence of TRPV1 on diabetes-induced alterations in thermal pain sensitivity. Mol Pain 2008;4:9
12. Migita K, Moriyama T, Koguchi M, et al. Modulation of P2X receptors in dorsal root ganglion neurons of streptozotocin-induced diabetic neuropathy. Neurosci Lett 2009;452:200–203
13. Xu GY, Li G, Liu N, Huang LY. Mechanisms underlying purinergic P2X3 receptor-mediated mechanical allodynia induced in diabetic rats. Mol Pain 2011;7:60
14. Burnstock G. Purinergic mechanosensory transduction and visceral pain. Mol Pain 2009;5:69
15. Burnstock G. Purinergic receptors and pain. Curr Pharm Des 2009;15:1717–1735
16. Burnstock G. Purinergic mechanisms and pain—an update. Eur J Pharmacol 2013;716:24–40
17. Tu WZ, Cheng RD, Cheng B, et al. Analgesic effect of electroacupuncture on chronic neuropathic pain mediated by P2X3 receptors in rat dorsal root ganglion neurons. Neurochem Int 2012;60:379–386
18. Lin J, Li G, Den X, et al. VEGF and its receptor-2 involved in neuropathic pain transmission mediated by $P2X_2(/)_3$ receptor of primary sensory neurons. Brain Res Bull 2010;83:284–291
19. Xu GY, Huang LY. Peripheral inflammation sensitizes P2X receptor-mediated responses in rat dorsal root ganglion neurons. J Neurosci 2002;22:93–102
20. Xu GY, Shenoy M, Winston JH, Mittal S, Pasricha PJ. P2X receptor-mediated visceral hyperalgesia in a rat model of chronic visceral hypersensitivity. Gut 2008;57:1230–1237
21. Wang C, Ning LP, Wang YH, et al. Nuclear factor-kappa B mediates TRPV4-NO pathway involved in thermal hyperalgesia following chronic compression of the dorsal root ganglion in rats. Behav Brain Res 2011;221:19–24
22. Sun T, Yu E, Yu L, Luo J, Li H, Fu Z. LipoxinA(4) induced antinociception and decreased expression of NF-κB and pro-inflammatory cytokines after chronic dorsal root ganglia compression in rats. Eur J Pain 2012;16:18–27
23. Shi L, Zhang HH, Xiao Y, Hu J, Xu GY. Electroacupuncture suppresses mechanical allodynia and nuclear factor κ B signaling in streptozotocin-induced diabetic rats. CNS Neurosci Ther 2013;19:83–90
24. Hargreaves K, Dubner R, Brown F, Flores C, Joris J. A new and sensitive method for measuring thermal nociception in cutaneous hyperalgesia. Pain 1988;32:77–88
25. Austin PJ, Wu A, Moalem-Taylor G. Chronic constriction of the sciatic nerve and pain hypersensitivity testing in rats. J Vis Exp 2012;(61):e3393
26. Thornton PD, Gerke MB, Plenderleith MB. Histochemical localisation of a galactose-containing glycoconjugate expressed by sensory neurones innervating different peripheral tissues in the rat. J Peripher Nerv Syst 2005;10:47–57
27. Qi F, Zhou Y, Xiao Y, et al. Promoter demethylation of cystathionine-β-synthetase gene contributes to inflammatory pain in rats. Pain 2013;154:34–45
28. Xu GY, Winston JH, Shenoy M, Zhou S, Chen JD, Pasricha PJ. The endogenous hydrogen sulfide producing enzyme cystathionine-beta synthase contributes to visceral hypersensitivity in a rat model of irritable bowel syndrome. Mol Pain 2009;5:44
29. Frommer M, McDonald LE, Millar DS, et al. A genomic sequencing protocol that yields a positive display of 5-methylcytosine residues in individual DNA strands. Proc Natl Acad Sci U S A 1992;89:1827–1831
30. Liu Y, Zhu H, Liu M, et al. Downregulation of Pax3 expression correlates with acquired GFAP expression during NSC differentiation towards astrocytes. FEBS Lett 2011;585:1014–1020
31. Chen YL, Law PY, Loh HH. Sustained activation of phosphatidylinositol 3-kinase/Akt/nuclear factor kappaB signaling mediates G protein-coupled delta-opioid receptor gene expression. J Biol Chem 2006;281:3067–3074
32. Viswaprakash N, Vaithianathan T, Viswaprakash A, Judd R, Parameshwaran K, Suppiramaniam V. Insulin treatment restores glutamate (α-amino-3-hydroxy-5-methyl-4-isoxazolepropionic acid) receptor function in the hippocampus of diabetic rats. J Neurosci Res 24 March 2015 [Epub ahead of print]. DOI: 10.1002/jnr.23589
33. Bishnoi M, Bosgraaf CA, Abooj M, Zhong L, Premkumar LS. Streptozotocin-induced early thermal hyperalgesia is independent of glycemic state of rats: role of transient receptor potential vanilloid 1(TRPV1) and inflammatory mediators. Mol Pain 2011;7:52
34. Gu JG, MacDermott AB. Activation of ATP P2X receptors elicits glutamate release from sensory neuron synapses. Nature 1997;389:749–753
35. Gu JG, Heft MW. P2X receptor-mediated purinergic sensory pathways to the spinal cord dorsal horn. Purinergic Signal 2004;1:11–16
36. Ho DH, Burggren WW. Epigenetics and transgenerational transfer: a physiological perspective. J Exp Biol 2010;213:3–16

37. Zhang Z, Cai YQ, Zou F, Bie B, Pan ZZ. Epigenetic suppression of GAD65 expression mediates persistent pain. Nat Med 2011;17:1448–1455
38. Turek-Plewa J, Jagodziński PP. The role of mammalian DNA methyltransferases in the regulation of gene expression. Cell Mol Biol Lett 2005;10:631–647
39. Bergman Y, Mostoslavsky R. DNA demethylation: turning genes on. Biol Chem 1998;379:401–407
40. Wang Y, Liu C, Guo QL, et al. Intrathecal 5-azacytidine inhibits global DNA methylation and methyl- CpG-binding protein 2 expression and alleviates neuropathic pain in rats following chronic constriction injury. Brain Res 2011;1418:64–69
41. Bird AP. CpG-rich islands and the function of DNA methylation. Nature 1986;321:209–213
42. Bogdanović O, Veenstra GJ. DNA methylation and methyl-CpG binding proteins: developmental requirements and function. Chromosoma 2009;118:549–565
43. Jurkowska RZ, Jurkowski TP, Jeltsch A. Structure and function of mammalian DNA methyltransferases. Chembiochem 2011;12:206–222
44. Okano M, Xie S, Li E. Cloning and characterization of a family of novel mammalian DNA (cytosine-5) methyltransferases. Nat Genet 1998;19:219–220
45. Karin M, Yamamoto Y, Wang QM. The IKK NF-kappa B system: a treasure trove for drug development. Nat Rev Drug Discov 2004;3:17–26
46. Yamamoto Y, Gaynor RB. IkappaB kinases: key regulators of the NF-kappaB pathway. Trends Biochem Sci 2004;29:72–79
47. Williams MD, Nadler JL. Inflammatory mechanisms of diabetic complications. Curr Diab Rep 2007;7:242–248
48. Hansen JM, Zhang H, Jones DP. Mitochondrial thioredoxin-2 has a key role in determining tumor necrosis factor-alpha-induced reactive oxygen species generation, NF-kappaB activation, and apoptosis. Toxicol Sci 2006;91:643–650
49. Berti-Mattera LN, Kern TS, Siegel RE, Nemet I, Mitchell R. Sulfasalazine blocks the development of tactile allodynia in diabetic rats. Diabetes 2008;57:2801–2808